Materials Science Forum
ISSN: 1662-9752, Vol. 1193, pp 47-54
doi:10.4028/p-3CfRaK
© 2026 The Author(s). Published by Trans Tech Publications Ltd, Switzerland.
Submitted: 2025-09-12
Revised: 2026-01-06
Accepted: 2026-03-21
Online: 2026-05-21

Correlation Study of Physical and Optical Total Thickness Variation in 4H-SiC Substrates

David M. Lynch[1,a*], Gregory L. Keaton[1,b], Christopher A. Lee[2,c] and Alexander T. Bean[3,d]

[1]Halo Industries, 3270 Scott Blvd., Santa Clara, CA 95054, USA

[2]Corning Incorporated, 60 O'Connor Rd., Fairport, NY 14450, USA

[3]Landmark Measurement Solutions Inc., 9990 Coconut Rd., Estero, FL 34135, USA

[a*]david.lynch@halo-industries.com, [b]greg@halo-industries.com, [c]leeca@corning.com, [d]alex@landmarkmeasurement.com

Keywords: total thickness variation (TTV), frequency scanning interferometry, refractive index homogeneity.

Abstract. Accurate total thickness variation (TTV) measurement is essential for silicon carbide (SiC) wafer manufacturing and process control. This work evaluates the accuracy of interferometric TTV measurements using the Corning Tropel FlatMaster MSP system, benchmarked against a dual-source chromatic white light (CWL) profilometer. We investigate the influence of spatial refractive index variation on interferometric accuracy by comparing MSP and CWL results. The analysis reveals high MSP repeatability with small deviations linked to index variation. These trends provide a framework for interpreting interferometric TTV data and improving metrology practices for SiC substrates.

Introduction

The rapid growth of power and optoelectronic devices has positioned silicon carbide (SiC) as a critical semiconductor valued for its wide bandgap, high thermal conductivity, and high breakdown field strength. As demand accelerates, particularly for larger-diameter substrates, efficient and scalable manufacturing becomes essential.

SiC wafer production faces persistent challenges. Mechanical wire sawing introduces kerf loss, residual stress, and geometric distortions such as bow, warp, and total thickness variation (TTV). Post-processing steps like grinding and chemical mechanical polishing (CMP) can mitigate these effects but add material loss. Emerging laser-based wafering methods aim to minimize kerf loss and stress-induced deformation; such approaches are under development by Halo Industries and others.

Accurate wafer geometry measurement is crucial for process control and device yield. Chromatic white light (CWL) profilometry provides direct thickness mapping by measuring both wafer surfaces, but its scanning nature limits speed and spatial resolution. Interferometric systems, such as the Corning Tropel FlatMaster MSP, enable rapid, full-field measurements with high sampling density [1, 2].

However, interferometry depends on the substrate's refractive index to convert optical path distance into physical thickness. Variations in index arising from doping or other local inhomogeneities introduce systematic errors. While these effects are recognized, existing studies of these dependencies are sparse and often restricted to single-wavelength data [3].

This work evaluates interferometric TTV measurements of 4H-SiC wafers on the MSP, benchmarked against a dual-source CWL profilometer. We quantify refractive index effects across both intentional doping levels (semi-insulating to heavily doped) and unintentional material variations (e.g., near basal facet regions). Results demonstrate high MSP repeatability and systematic deviations linked to index variation, offering more robust TTV metrology in SiC manufacturing.

This article is an open access article under the terms and conditions of the Creative Commons Attribution (CC BY) license (https://creativecommons.org/licenses/by/4.0)

Experimental Plan

Samples.

We analyzed the thickness and optical properties of 4H-SiC wafers fabricated by Halo Industries' laser-based wafering method. Most samples were 150 mm device-grade n-type wafers (N-doped, 19-24 mΩ·cm) with a 4° miscut toward [11$\bar{2}$0]; five were 200 mm optical-grade, undoped, and without miscut.

Measurement Methods.

Interferometric thickness was measured by frequency-scanning interferometry on a Corning Tropel FlatMaster MSP 300 with an 830 nm laser. Results were benchmarked against physical thickness measured using a Camtek FRT Microprof MHU, equipped with dual chromatic white light (CWL) sensors for simultaneous mapping of the top and bottom surfaces.

The MSP collects 128 interferograms while stepping the laser from 825–835 nm. A Fourier transform yields spectra with peaks from different surface pairs [Fig. 1(a)]. The location of each peak in Fourier space gives the optical path difference (OPD) between the two surfaces, where the OPD is defined as:

$$OPD = n_g \cdot t \tag{1}$$

where n_g is the group index and t is the distance between surfaces. Therefore, the Fourier spectrum can be used to calculate the thickness of the sample if the group index is known. Since illumination is nearly parallel to the crystallographic c-axis, the ordinary group index is appropriate for MSP thickness calculations [5, 6]. For initial calculations, we assumed an n_g of 2.690, and any residual index error was corrected by calibration against CWL thickness measurements:

$$n_{cal} = n_{used} \cdot \frac{t_{MSP}}{t_{CWL}} \tag{2}$$

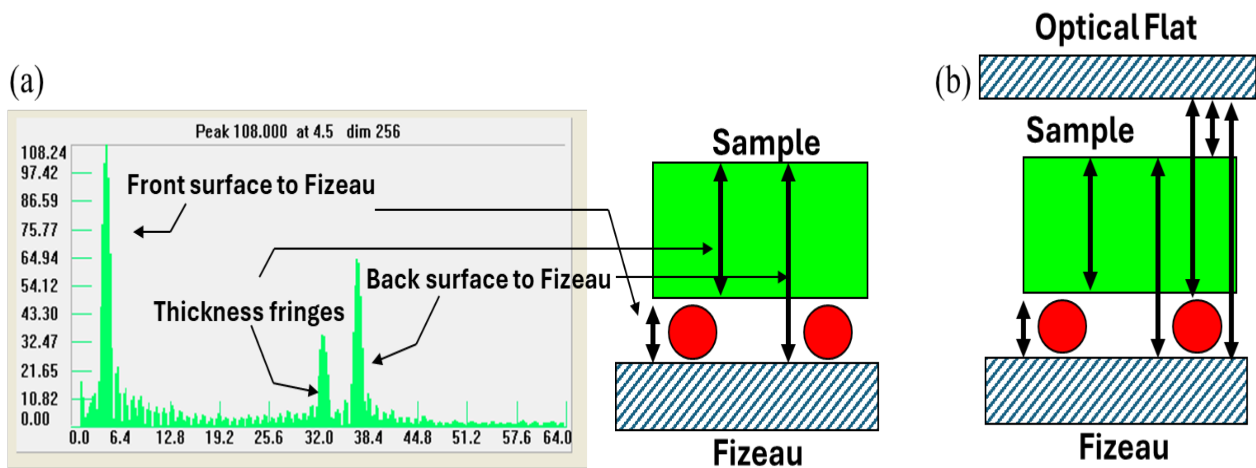

Fig. 1. (a) Schematic of the MSP measurement [4]. Fourier spectrum of the interference patterns shows peaks from different surface pairs. (b) MSP stack with an optical flat, enabling independent measurement of wafer thickness and group index via additional surface pairs.

Refractive Index Verification.

Refractive index verification was performed using two independent methods. Phase index was measured at 632.8 nm with a Metricon prism-coupler (TE-polarized HeNe laser). Group index at 950 nm was measured on a custom MSP with a 950 nm laser and optical flat [Fig. 1(b)], enabling independent determination of thickness and index.

Optical Retardance.

Optical retardance maps were collected with an Ilis StrainScope Stepper 200. For doped wafers with a 4° tilt, samples were physically tilted ~12° toward $[11\bar{2}0]$ to align with the optic axis and suppress intrinsic birefringence. The measured retardance therefore primarily reflects stress-induced birefringence.

MSP vs. CWL Thickness Measurements

Measurement Overview.

Fig. 2(a) shows an MSP thickness map of a CMP-processed 150 mm doped wafer measured in ~30 s (340 µm average thickness, 170 µm pixel size, ~600k points). This combination of speed and dense sampling highlights the strength of interferometry for full-wafer metrology.

Nanotopography maps can be generated directly from MSP data by removing low-order Zernike terms and applying a Gaussian filter [Fig. 2(b)]. This reveals sub-micron features (±200 nm here) that are otherwise obscured in the raw map, such as radial patterns from residual grinding damage and concentric CMP artifacts. The ability to extract these details rapidly from high-resolution wafer-level maps is a key advantage of the MSP approach.

By contrast, CWL profilometry achieves direct physical thickness mapping without index assumptions but at the cost of throughput. Fig. 2(c) shows a CWL map of comparable resolution (341 µm average thickness, 100 µm pitch), which required ~90 minutes per wafer. To reduce acquisition time to ~10 minutes, the measurement pitch must be coarsened to 1.5 mm (~8k points), as in Fig. 2(d), but this sacrifices spatial detail.

These examples illustrate a fundamental trade-off: CWL provides direct thickness but only with slow, step-and-scan measurements, while MSP delivers fast, high-resolution maps suitable for wafer-level process control. This contrast is expected to become even more pronounced at larger wafer diameters, underscoring the scalability advantage of interferometric metrology.

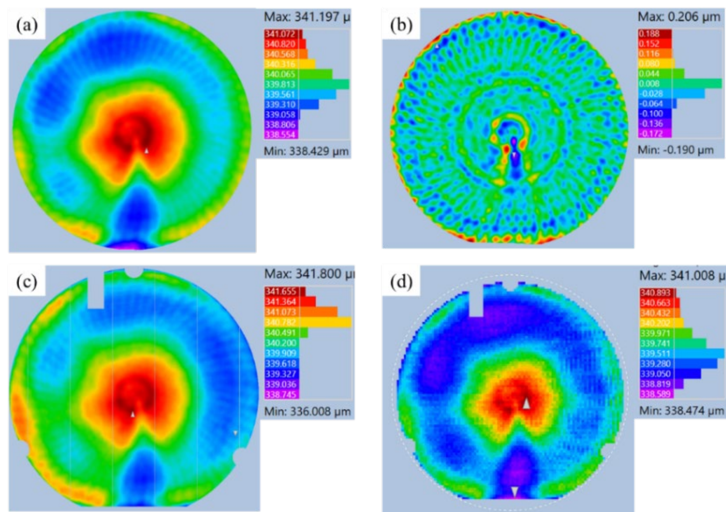

Fig. 2. Example thickness maps for a 150 mm wafer: (a) MSP thickness map, (b) MSP nanotopography map (Gaussian-filtered with cutoff wavelength of 20 mm), (c) high-resolution CWL map, and (d) low-resolution CWL map.

Refractive Index Calibration.

MSP thickness relies on the assumed refractive index. At a given OPD measurement,

$$t = \frac{OPD}{n_g} \tag{3}$$

so a small index error Δn_g produces a thickness error

$$\Delta t = -\frac{t}{n_g}\Delta n_g \quad (4)$$

Thus, thickness error scales with wafer thickness and the fractional index error. Table 1 shows that a 1/1000 index error yields ~100–200 nm thickness error. While modest, larger index deviations can quickly become significant.

Table 1. Estimated thickness error from a 1/1000 error in assumed group index, evaluated for nominal wafer thicknesses at $n_g = 2.690$.

n_g	Wafer Thickness [µm]	Δt [nm] ($\Delta n_g = 0.001$)
2.690	350	130
	500	186

A simple calibration method is to compare MSP average thickness with physical thickness from CWL. Fig. 3 shows this relationship for doped wafers, with a fit slope giving

$$\frac{t_{MSP}}{t_{CWL}} = \frac{n_{cal}}{n_{used}} = 1.00066 \quad (5)$$

indicating a ~0.07% overestimation and suggesting a true index of 2.692 (vs. 2.690).

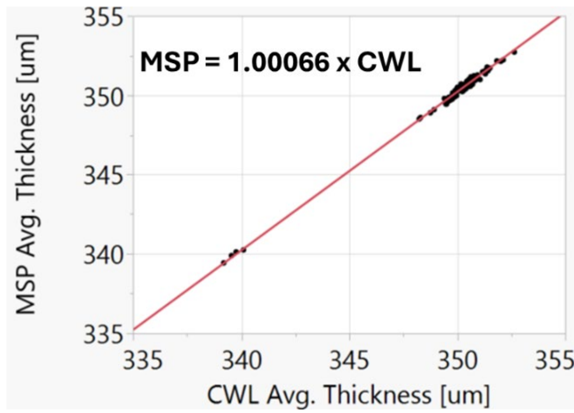

Fig. 3. MSP vs. CWL average thickness for doped wafers, with proportional fit showing a ~0.07% overestimation of MSP thickness with a chosen index of 2.690.

While global averages provide a quick calibration, they can be skewed by outliers or macroscopic distortions (e.g., dimples, residual grind marks). To mitigate these effects, we instead compared full wafer maps by subtracting CWL and MSP thickness data after alignment and pixel matching [Fig. 4]. Although this approach can still be influenced by misalignment, edge exclusion differences, and CWL artifacts, the average value of the resulting difference maps offers a more robust estimate of index miscalibration.

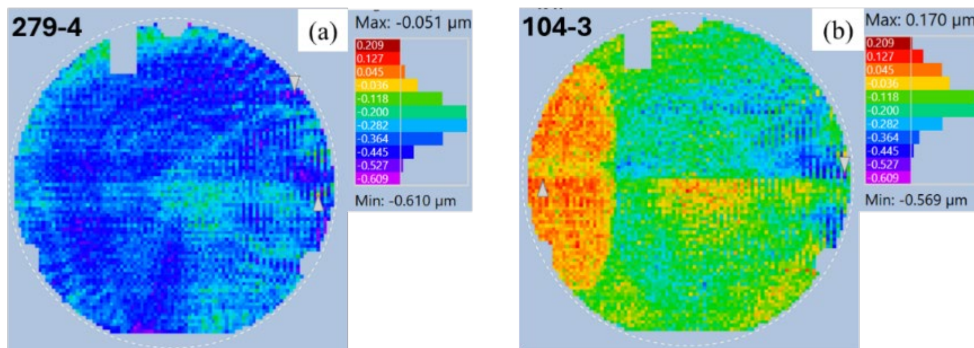

Fig. 4. Difference maps (CWL – MSP) for two wafers: (a) 279-4, variation mainly from map misalignment; (b) 104-3, variation dominated by basal facet region.

Table 2 summarizes mean difference map values by material type and source. Doped wafers showed consistent offsets of -210 to -250 nm across three suppliers, corresponding to calibrated indices of 2.691–2.692. Optical-grade wafers showed +310 nm average difference, corresponding to 2.688. These values imply ~0.04-0.07% systematic error in calculated thickness.

Table 2. Mean values of difference map averages by material source and type, with corresponding calibrated group index.

Material Source	Material Type	Difference Average [µm]	n_{cal}
A	Doped	-0.2476	2.692
B	Doped	-0.2169	2.691
C	Doped	-0.2351	2.692
D	Optical	0.3064	2.688

Refractive Index Uniformity.

Difference maps also reveal the spatial uniformity of the group index. While average offsets support global calibration, the standard deviation and range of the maps quantify local variation within each wafer [Fig. 5].

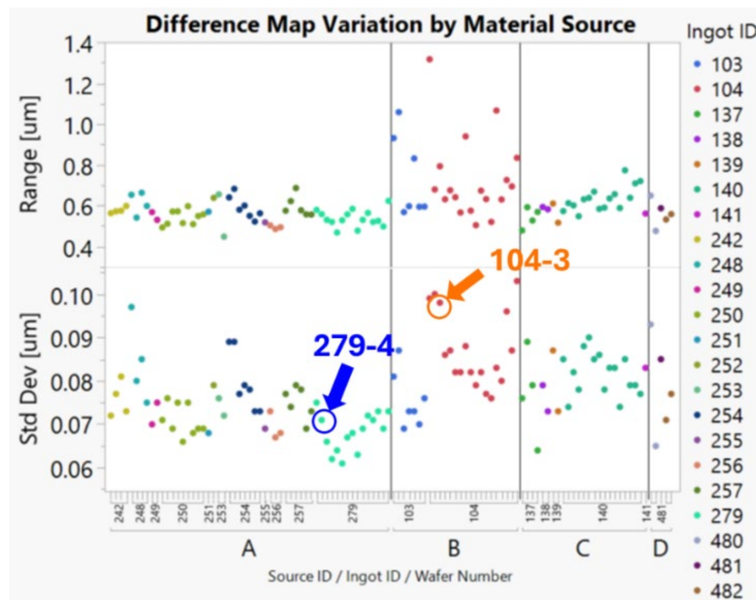

Fig. 5. Variation in wafer difference maps, shown as range (top) and standard deviation (bottom). Data are grouped by source (A–C: doped; D: optical), ingot ID, and wafer ID. Wafers from Fig. 4 are highlighted.

Across all wafers, the variation shows a noise floor of ~70–80 nm in standard deviation and 0.5–0.7 µm in range. This baseline largely reflects scan artifacts (e.g., the horizontal feature in Fig. 4(b)) and residual misalignment between MSP and CWL maps. Wafer 279-4 [Fig. 4(a)] illustrates this baseline: its minimal within-wafer variation demonstrates the agreement achievable between MSP and CWL thickness in the absence of material inhomogeneities.

Excursions above this floor point to spatially varying optical effects not explained by measurement artifacts. These deviations are typically linked to microstructural features that alter the index. For wafer 104-3 [Fig. 4(b)], the basal facet region appears 100–200 nm thicker than the wafer bulk. Nanotopography maps [Fig. 6] confirm this is not true thickness variation: the facet appears in the thickness map but not in the Si-face topography. This indicates an optical artifact caused by index variation, corresponding to a local index ~0.001 lower than the bulk value.

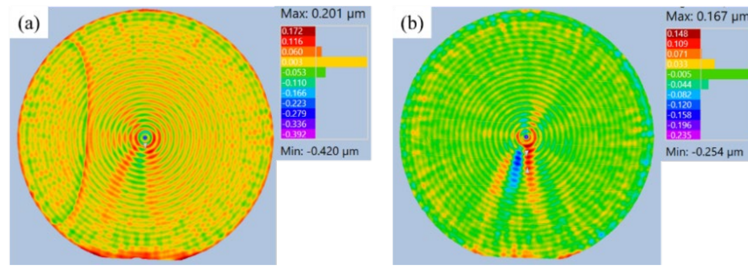

Fig. 6. Wafer 104-3 (a) thickness nanotopography and (b) Si face Nanotopography maps. The basal facet appears in (a) but not in (b), indicating an optical artifact rather than a true thickness variation.

Index Validation Measurements

Prism Coupling.

To independently assess the bulk index observed with MSP measurements, we performed prism-coupling measurements on selected wafers using TE-polarized light at 632.8 nm. This provides the ordinary phase index, the most relevant parameter since MSP primarily probes this direction under normal incidence. Results for doped and optical-grade wafers, including basal facet regions where available, are shown in Fig. 7 and summarized in Table 3. Measured indices agree with literature values [5] to within 0.04%.

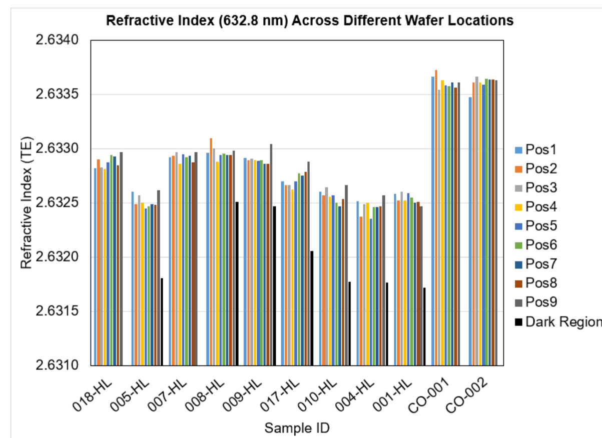

Fig. 7. In-plane refractive index measured by prism-coupling refractometry at 632.8 nm for select wafers at multiple radial positions. The first nine samples are doped wafers (with basal facet measurements labeled "Dark Region"); the final two are optical-grade wafers.

Table 3. Literature and measured ordinary refractive index at 632.8 nm [5].

<table>
<tr><td colspan="2">Literature Phase Index (o-ray)</td><td>2.634</td></tr>
<tr><td rowspan="3">Measured</td><td>Doped Bulk</td><td>2.633</td></tr>
<tr><td>Doped Basal</td><td>2.632</td></tr>
<tr><td>Optical Bulk</td><td>2.634</td></tr>
</table>

Measured index showed excellent uniformity across wafers, with typical within-wafer variations of ±0.0001, corresponding to ±20 nm effective thickness error in interferometric measurements. Localized deviations were observed in basal facet regions, where the index was reduced by ~0.001: an order of magnitude larger than bulk variation. This corresponds to a thickness error of ~130 nm, consistent with estimates from wafer 104-3 [Fig. 4]. These results confirm that basal facets introduce small but measurable refractive index shifts, which can impact MSP-derived TTV.

Interferometry.

Difference maps provide useful insight, but they are limited by CWL resolution and scan/alignment artifacts. These limitations can be avoided by measuring index-independent thickness directly on the

MSP using the configuration shown in Fig. 1(b). Inserting an optical flat introduces additional surface pairs in the measurement stack, allowing both OPD and thickness to be independently measured. From these, an index map can be calculated across the wafer. Examples are shown in Fig. 8 for a doped wafer with a basal facet and for an optical-grade wafer.

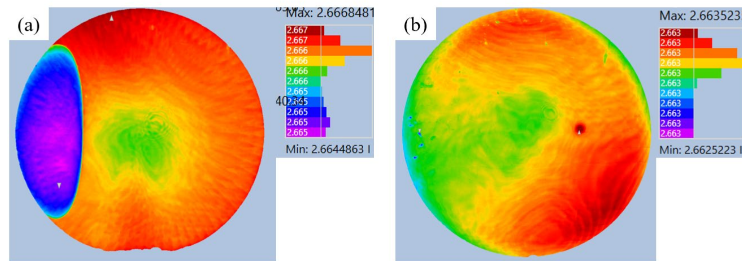

Fig. 8. Group index maps measured with an MSP at 950 nm using the configuration in Fig. 1(b). (a) Doped wafer 104-4, showing a large basal facet region with lower index than the wafer bulk. (b) Optical-grade wafer with highly uniform index.

The doped wafer [Fig. 8(a)] exhibits a bimodal index distribution: 2.665 in the basal facet region and 2.666 in the wafer bulk (Table 4). These measurements, performed at 950 nm, differ slightly from earlier 830 nm data. The lower basal index is consistent with preferential dopant incorporation on basal facets during growth; n-type SiC index decreases with nitrogen concentration [7]. Using a single global index would introduce a ~130 nm thickness error, consistent with prism-coupling estimates.

Table 4. Literature and measured group index from the difference map method (830 nm) and optical flat method (950 nm) [5].

		Wavelength	
		830 nm	950 nm
Literature Group Index (o-ray)		2.692	2.661
Measured	**Doped Bulk**	2.692	2.666
	Doped Basal	2.688	2.665
	Optical Bulk	2.688	2.663

In contrast, the optical-grade wafer [Fig. 8(b)] shows high uniformity, with an average index of 2.663 and standard deviation of 0.0001. This corresponds to a ±20 nm thickness error, indicating that a single calibrated global index can yield accurate thickness for high-quality optical wafers.

Optical Retardance.

Intrinsic stress in the SiC crystal manifests as stress-induced birefringence, which can be quantified and visualized [8, 9]. Optical retardance maps for the wafers in Fig. 8 (rotated 90°) highlight stress-induced birefringence. For the doped wafer, a 12° tilt was applied to suppress intrinsic birefringence, isolating stress contributions. The map reveals a radial stress field: the center is nearly stress-free, while edges show stronger radial alignment. The maximum retardance (~12 nm) corresponds to a birefringence of 3×10^{-5} for a 350 μm wafer: an order of magnitude smaller than the index variations measured with the MSP. The optical-grade wafer shows a similar maximum birefringence (2×10^{-5} for 500 μm wafer), but with improved uniformity, as most of the wafer remains at ~4×10^{-6}.

This contrast indicates that stress in doped material is more localized and directional, whereas optical-grade material remains low, homogeneous stress. Although these stress signatures are small compared to index variation, they may reflect wafer thermal or mechanical history. Radial patterns could originate from growth gradients, while reduced stress in optical-grade material suggests improved processing. Further correlation of retardance with growth conditions and yield could clarify their significance.

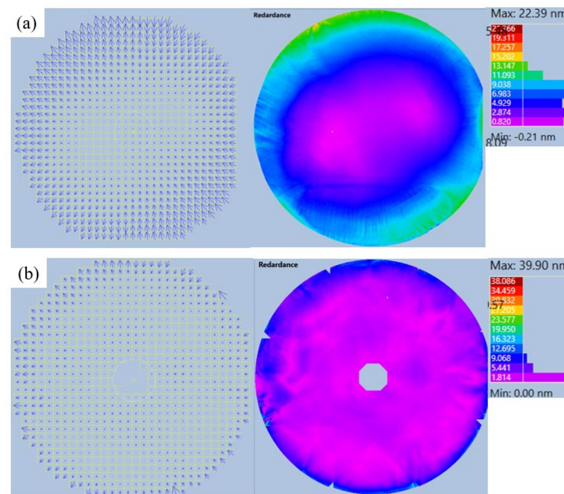

Fig. 9. Optical retardance maps of wafers from Fig. 8 shown as vector maps and heat maps (retardance in nm). (a) Doped wafer with a radial stress field and higher edge retardance. (b) Optical-grade wafer with improved retardance uniformity (central data missing in stitched map).

Summary

The MSP provides rapid, high-resolution wafer measurements with excellent repeatability, far exceeding CWL throughput. Bulk refractive index uniformity was stable, introducing only ±20 nm thickness error when a single global index is applied, and localized deviations near basal facets produced errors ~100–200 nm. Though small relative to wafer thickness, these effects show that local inhomogeneities can bias results if overlooked. MSP offers a robust, scalable approach for SiC wafer metrology if index calibration and awareness of local variations are maintained.

References

[1] J. Wang *et al.*, Optical characterization of high refractive index glass wafers for augmented reality wearables, Optical Interference Coatings Conference (2019).

[2] T. Dunn, C. Lee, M. Tronolone, and A. Shorey, Characterization of wafer thickness uniformity during 3D-IC processing, IEEE 62nd Electronic Components and Technology Conference (2012).

[3] G. Lim, T. Manzur, and A. Kar, Improved optical properties and defectivity of an uncooled silicon carbide mid-wave infrared optical detector with increased dopant concentration, J. Opt. 14, (2012) 105601.

[4] FlatMaster MSP for augmented reality waveguides, Corning Tropel Applications (2019).

[5] S. Wang *et al.*, 4H-SiC: A new nonlinear material for infrared lasers, Laser Photonics Rev. 7 (2013) 831-838.

[6] "Effective index", Sellmeier coefficients, and glass thickness measurements on FM-MSP, Corning Tropel Applications (2024).

[7] T. Bosma *et al.*, Broadband single-mode planar waveguides in monolithic 4H-SiC, J. Appl. Phys. 131(2) (2022) 025703.

[8] K. Gomi *et al.*, Residual stress estimation in SiC wafer using IR polariscope, 2008 International Conference on Electronic Materials and Packaging (2008).

[9] V. Ganapati *et al.*, Infrared birefringence imaging of residual stress and bulk defects in multicrystalline silicon, J. Appl. Phys. 108 (2010) 063528.